



HAL
open science

Analysis of micro-dispersed PCM-composite boards behavior in a buiding's wall for different seasons

Kamal El Omari, Yves Le Guer, Pascal Bruel

► To cite this version:

Kamal El Omari, Yves Le Guer, Pascal Bruel. Analysis of micro-dispersed PCM-composite boards behavior in a buiding's wall for different seasons. *Journal of Building Engineering*, 2016, 7, pp.11. 10.1016/j.jobe.2016.07.013 . hal-01353957

HAL Id: hal-01353957

<https://inria.hal.science/hal-01353957>

Submitted on 20 Apr 2024

HAL is a multi-disciplinary open access archive for the deposit and dissemination of scientific research documents, whether they are published or not. The documents may come from teaching and research institutions in France or abroad, or from public or private research centers.

L'archive ouverte pluridisciplinaire **HAL**, est destinée au dépôt et à la diffusion de documents scientifiques de niveau recherche, publiés ou non, émanant des établissements d'enseignement et de recherche français ou étrangers, des laboratoires publics ou privés.

Author's Accepted Manuscript

Analysis of micro-dispersed PCM-composite boards behavior in a building's wall for different seasons

Kamal EL OMARI, Yves LE GUER, Pascal BRUEL



PII: S2352-7102(16)30111-5
DOI: <http://dx.doi.org/10.1016/j.job.2016.07.013>
Reference: JOBE161

To appear in: *Journal of Building Engineering*

Received date: 2 February 2016
Revised date: 11 May 2016
Accepted date: 31 July 2016

Cite this article as: Kamal EL OMARI, Yves LE GUER and Pascal BRUEL
Analysis of micro-dispersed PCM-composite boards behavior in a building's wall
for different seasons, *Journal of Building Engineering*
<http://dx.doi.org/10.1016/j.job.2016.07.013>

This is a PDF file of an unedited manuscript that has been accepted for publication. As a service to our customers we are providing this early version of the manuscript. The manuscript will undergo copyediting, typesetting, and a review of the resulting galley proof before it is published in its final citable form. Please note that during the production process errors may be discovered which could affect the content, and all legal disclaimers that apply to the journal pertain

Analysis of micro-dispersed PCM-composite boards behavior in a building's wall for different seasons

Kamal EL OMARI^{a,*}, Yves LE GUER^a, Pascal BRUEL^b

^a*Université de Pau et des Pays de l'Adour (UPPA),
Laboratoire des Sciences de l'Ingénieur Appliquées à la Mécanique et au génie électrique (SIAME),
64000 Pau, France.*

^b*CNRS - Laboratoire de Mathématiques et de leurs Applications,
Inria Cagire Team, 64000 Pau, France.*

Abstract

The integration of phase change materials (PCMs) in buildings especially in their walls is the subject of more than a decade of growing interest due to their potentialities for energy saving and enhancement of thermal comfort. The present investigation concerns the applications related to thermal insulation. The idealized composite wall considered here numerically can be thought of as resulting from the incorporation of shape-stabilized PCM particles in a polymer matrix. A novel model is developed to study the thermal behavior of this PCM-composite when used as a planar insulating material submitted to variable thermal modulations on one of its faces. The numerical model couples the heat transfer in the wall with the heat transfer and the crystallization/melting process within PCM inclusions considered as spherical. Both processes are modeled by a finite volume approach combined with the enthalpy method to account for the phase change. Simulation results are used to monitor the temperatures in the wall and quantify the energy exchanges between its two sides. The thickness of the wall and the volume fraction of the incorporated PCM were varied in this study. This analysis permits to point out the configurations for which the negative effect of the higher thermal conductivity of the PCM outweighs the benefits related to its latent heat. The analysis is extended to different external temperature modulations representing different typical seasons/climates. The results show the impact of the choice of the PCM phase change temperature on the wall thermal efficiency over the year. For the case investigated, it was shown that a PCM composite board with increased performances during a summer day exhibits a degraded behavior during a winter day when compared to a pure (without PCM) insulation material.

*Corresponding author.

32 *Keywords:* Phase change material (PCM), composite board, dispersed PCM, building
33 thermal insulation, enthalpy method.

34 **1. Introduction**

35 It is widely accepted that buildings and particularly those dedicated to housing repre-
36 sent a significant potential for energy saving, mainly related to the use of heating and air
37 conditioning systems [1, 2, 3]. In that domain, the objective of the research and devel-
38 opment community is to develop innovative approaches to save energy while preserving
39 if not enhancing the thermal comfort of the buildings' inhabitants. In that framework,
40 quite a significant number of recent studies focused on the use of phase change materials
41 (PCMs) in buildings. They can be used as standalone systems to store energy, embedded
42 in the structure [4, 5, 6] or in the external envelope [7, 8, 9]. The integration of PCMs re-
43 sults in an increase of the building thermal inertia, especially for lightweight construction.
44 Combined with an efficient insulating material, it helps to reduce the indoor temperature
45 peaks related to the outdoor temperature evolution and the solar radiation received at the
46 external facades. Different techniques allow the integration of PCMs in building envelope
47 materials: impregnation, incorporation of micro-encapsulations or macro-encapsulation in
48 the form of slabs for example [10, 11, 12]. These solutions have attracted a great interest
49 and have been the subject of a significant number of both numerical and experimental
50 studies [13, 14, 15, 16, 17, 18]. There exist also encapsulation free techniques based on the
51 direct incorporation of the PCM during the fabrication process or on immersion methods
52 for natural porous materials [19]. For PCM-composite boards based on natural polymer
53 matrices, one promising method involves the use of the low-energy emulsification tech-
54 nique [20, 21]. Since the plain insulation panels e.g. PCM-free commercially available
55 have standardized thicknesses, the development of a PCM-composite board offering the
56 same thickness range seems a reasonable choice. But even the choice of the proper PCM
57 to be incorporated in a given matrix is not straightforward though. First, because of its
58 relatively high conductivity when compared to that of the matrix, the overall thermal
59 behavior of the PCM-composite board may be degraded under certain conditions when
60 compared to that of its PCM free counterpart. Second, a melting temperature suitable for
61 high outdoor temperatures (e.g. summer days) may lead to poor performances for lower
62 external temperatures (e.g. winter days). Since a case by case analysis will ultimately

63 discriminate between the possible combinations of parameters, the availability of physical
64 models that permits to discriminate a priori between the different possible alternatives
65 is highly desirable. Accordingly, the goal of the present study is to propose such a nu-
66 merical model and to illustrate for generic situations how it can be used to analyze the
67 overall thermal effectiveness of a PCM-composite board and compare it with that of a
68 plain board of the same thickness. This contribution is organized as follows: first, the
69 proposed model and the method of solution are presented and validated. Then, the model
70 is applied to the academic configuration of a harmonic external temperature modulation
71 around the melting temperature chosen equal to the indoor temperature. The sensitivity
72 to the nature of the insulating matrix is investigated by considering a more conductive
73 material (i.e. cement). The case of a non-smooth harmonic modulation of the outdoor
74 temperature is also investigated to evidence the effect of small-scale perturbations. Fi-
75 nally, the results obtained for a more realistic but still idealized external temperature
76 evolution representative of either a summer or winter generic day are discussed.

77 2. Numerical Modelling

78 2.1. Physical model and assumptions

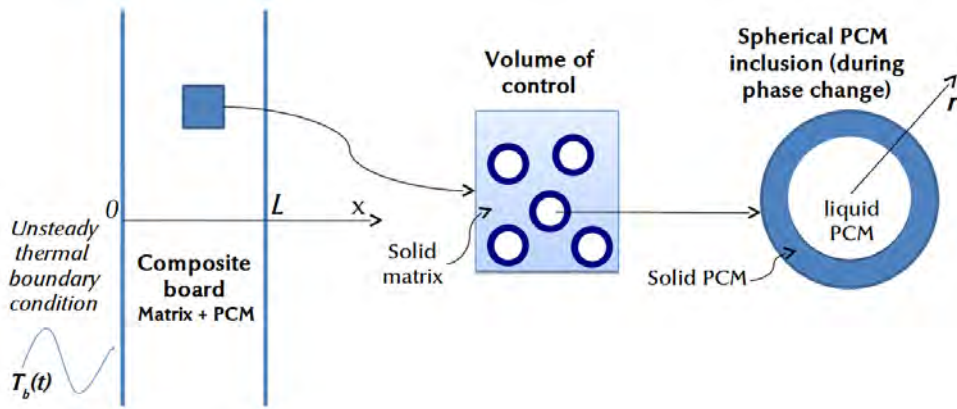


Figure 1: Sketch of the modelled system: the composite board and a volume of control containing PCM spheres undergoing phase change.

79 The unsteady thermal behavior of an insulation board containing microscopic spherical
80 inclusions of a PCM is investigated. The diameter of the monodisperse PCM particles
81 is $d = 100 \mu\text{m}$ [21]. The PCM spheres are homogeneously dispersed in a solid matrix
82 (see Fig. 1). The wall has a relatively small thickness compared to its lateral dimensions

83 which allows us to use a one-dimensional model for the heat transfer through it. The heat
84 transfer model considers thermal conduction in the matrix and thermal conduction inside
85 the PCM inclusions along with melting and crystallization phenomena combined with an
86 appropriate boundary condition at the interface. As the inclusions are small in diameter
87 (100 μm), the natural convection inside these PCM inclusions is not taken into account
88 when they are in liquid state (i.e. the Rayleigh number is well below 1). In the equation
89 of heat governing the thermal transfer in the wall, appears a source term Φ_i corresponding
90 to the power exchanged between the solid matrix and the PCM spheres, namely:

$$\int_{V_i} (1 - \phi)(\rho c_p) \frac{\partial T}{\partial t} dV = \int_{S_i} k_{\text{eff}} \vec{\nabla} T \cdot \vec{d}S + \Phi_i \quad (1)$$

91 where V_i is a control volume within the matrix surrounded by a surface S_i . ϕ is the volume
92 fraction of PCM contained in a control volume V_i . The source term Φ_i representing the
93 heat flux exchanged between the spheres and the matrix of volume $(1 - \phi)V_i$ is detailed
94 below. The effective thermal conductivity of the composite k_{eff} that appears in Eq. (1)
95 was estimated using the Maxwell's model [22]:

$$k_{\text{eff}} = k_m \frac{k_d + 2k_m + 2\phi(k_d - k_m)}{k_d + 2k_m - \phi(k_d - k_m)}. \quad (2)$$

96 where k_d is the thermal conductivity of the dispersed PCM as given by Eq. 5 and k_m
97 corresponds to average value of the thermal conductivity for the whole matrix.

98 The finite volume method is used to resolve Eq. (1). Thus, the thickness of the wall
99 is divided into N control volumes of gradual increasing size $\{V_i, i = 1 \rightarrow N\}$ (from the
100 boundary to the center). The number of inclusions in a control volume is [23]:

$$\Lambda_i = \frac{6\phi V_i}{\pi d^3} \quad (3)$$

101 where d stands for the diameter of the spheres.

102 The Λ_i spheres in each control volume are identical and are supposed to follow the
103 same thermal or phase change process, thus, a unique sphere is modeled per control
104 volume, representing the kinetics of the other spheres. The ‘‘enthalpy’’ finite volume
105 method is used to model the heat transfer with phase change within the N different
106 spheres. This method is based on an enthalpy formulation of the heat equation (used
107 here in its temperature form) applied to both liquid and solid phases. Thus, a unique
108 mesh (or grid) cover the two media (liquid and solid). The kinetics of the phase change

109 (freezing or melting) is related to the evolution of the liquid phase fraction f of the PCM.
 110 The heat equation inside the spheres reads as:

$$\int_{v_i} (\rho c_p)_d \frac{\partial T}{\partial t} dv = \int_{s_i} k_d \vec{\nabla} T \cdot \vec{ds} - \int_{v_i} \rho_d L_m \frac{\partial f}{\partial t} dv \quad (4)$$

111 The model is unidimensional, formulated in spherical coordinates. The spheres are divided
 112 into M equal control volumes (the radius is unequally divided). v_i is the control volume
 113 delimited by the two spheres of radii r_i and r_{i-1} . Only the central volume ($i = 0$) has a
 114 spherical shape. The last term of Eq. (4) accounts for the evolution of the local liquid
 115 fraction in the control volume v_i . The properties Ψ (density, thermal conductivity and
 116 specific heat) of the dispersed PCM are calculated as:

$$\Psi_d = f \Psi_{MCP}^{\text{liquid}} + (1 - f) \Psi_{MCP}^{\text{solid}}. \quad (5)$$

117 The boundary condition for this model is of Dirichlet type at the sphere surface, i.e.
 118 the instantaneous temperature of the control volume of the composite board containing
 119 the sphere is imposed at the outer surface of this sphere. In the other hand, two types of
 120 boundary conditions are applied to the wall. At one side of the composite board ($x = 0$),
 121 a generic unsteady boundary condition is applied. Considering the diversity of possible
 122 external conditions (external convection and radiative exchanges), a sinusoidal evolution
 123 of the external wall temperature is imposed. This behaviour is representative of what is
 124 experimentally observed for example by Ismail and Castro (see Fig. 17 of [13]) and is
 125 expressed as:

$$T(x = 0, t) = \bar{T} - A \sin(2\pi t/\tau) \quad \text{with } \tau = 1 \text{ day}. \quad (6)$$

126 At the other side of the board ($x = L$), a steady convective boundary condition is
 127 applied with a heat transfer coefficient $h = 10 \text{ W/m}^2 \text{ }^\circ\text{C}$:

$$k_{\text{eff}} \left. \frac{\partial T}{\partial x} \right|_L = h [T_\infty - T(L, t)] \quad \text{at } x = L. \quad (7)$$

128 This condition is a simplified representation of the behavior of an indoor medium main-
 129 tained at a fixed temperature T_∞ by an air conditioning system for example (heating
 130 and/or cooling).

131 *2.2. Numerical algorithms*

132 In the scope of the present study, the supercooling phenomenon is neglected and the
 133 PCM is considered as a pure material melting at a fixed temperature T_m . This assumption
 134 can be justified by the fact that low degrees of supercooling are obtained for slow cooling
 135 rates [24] as it is the case for daily periodically changing temperatures. Furthermore, the
 136 addition of nucleating agent in the PCM can reduce the degree of supercooling which is
 137 crucial for the heat storage application. Thus, the phase change front is modeled as a thin
 138 interface (1 grid cell having $0 < f < 1$). The modeling of the progression of this front
 139 coupled to the update of the liquid fraction field f is achieved using the “new source”
 140 algorithm of Voller [25]. The field of f is updated iteratively within each time step [26],
 141 in this way, the updated value of f_i^{k+1} at iteration $k+1$ and control volume i is calculated
 142 as follows:

$$f_i^{k+1} = f_i^k + \frac{dt a_i^k}{\rho L_m v_i} (T_i - T_m), \quad (8)$$

143 where a_i^k is the coefficient of T_i in the discretized version of Eq. (4). This update is
 144 followed by an overshoot/undershoot correction:

$$f_i^{k+1} = \begin{cases} 0 & \text{if } f_i^{k+1} < 0 \\ 1 & \text{if } f_i^{k+1} > 1. \end{cases} \quad (9)$$

145 To easily ensure that the temperature at the phase change front is equal to the melting
 146 temperature T_m , the energy equation is penalized at the computational cells belonging to
 147 the phase change front ($0 < f_i < 1$). This procedure is performed by adding a penalization
 148 source term, equal to $10^9 \times T_m$, to the RHS term of energy equations corresponding to
 149 these cells. This practice accelerates the convergence of the f updating algorithm, and
 150 the number of iterations needed to reach convergence ($|f_i^{k+1} - f_i^k| < \varepsilon_f$) may be lowered
 151 to 2 or even 1 depending on the size of the mesh and the time-step value. The value of
 152 the tolerance ε_f was fixed to 10^{-4} .

153 The spatial discretization of Eqs.(1) and (4) relies on centered difference schemes with
 154 second order accuracy, while the time scheme is implicit and first order. The Thomas
 155 algorithm is used to resolve the resulting tridiagonal linear system. The time step size
 156 dt has to be sufficiently small $dt \lesssim 10^{-3}$ s to ensure a strong coupling between the two
 157 models (matrix and spheres models). For the different configurations (different board
 158 thicknesses L , different PCM fractions ϕ), sufficiently fine grids were used to ensure the

159 grid independence of the results. These values were chosen after the mesh size and time
 160 step dependency studies presented in the next section. Thus, a wall of thickness $L = 5\text{cm}$
 161 was typically divided into $N = 80$ control volumes, while $M = 20$ was used for the spheres.
 162 Initially, the whole composite material was considered at a uniform temperature slightly
 163 higher than T_m , thus the whole PCM was at the liquid state $f = 1$.

164 The coupling algorithm between the different models (the board and sphere models)
 165 proceeds as follows:

166 **Step 1:** At each time step, the N phase change models (sphere models, Eq. 4) are
 167 advanced in time for a duration of dt .

168 **Step 2:** The heat flux at the spheres surface is calculated as:

$$\varphi_i = k_d \left. \frac{\partial T}{\partial r} \right|_{r=d/2} \quad (10)$$

169 **Step 3:** Φ_i , the source term of Eq. (1), is then calculated as:

$$\Phi_i = \Lambda_i \varphi_i (\pi d^2). \quad (11)$$

170 **Step 4:** Eq. (1) is then resolved for the same time step and the new temperatures of
 171 the N control volumes are obtained. These temperatures will be used as the new
 172 boundary conditions for the next time step (**Step 1**).

173 This loop cycle is repeated until convergence is reached.

174 2.3. Consistency test, mesh size dependency study and model validation

175 The model described above takes into account intrinsically both latent and sensible
 176 heat of the PCM. To check its consistency, the following test calculation was carried out:
 177 a wall containing $\phi = 20\%$ of spherical inclusions, having the same properties as those
 178 of the matrix, is considered and its thermal behavior is compared to that of a solid wall
 179 ($\phi = 0$). Both simulations should yield exactly the same results. The thickness of the
 180 wall is $L = 50\text{ mm}$, its properties are those listed in Table 2 and the indoor conditions
 181 are the same as in section 3.1. When the temperature of the left boundary varied over
 182 time according to Eq. (6), but without crossing the melting temperature of the PCM,
 183 (which was modified for this purpose to avoid phase change: $T_m = 0\text{ °C}$ for example), a

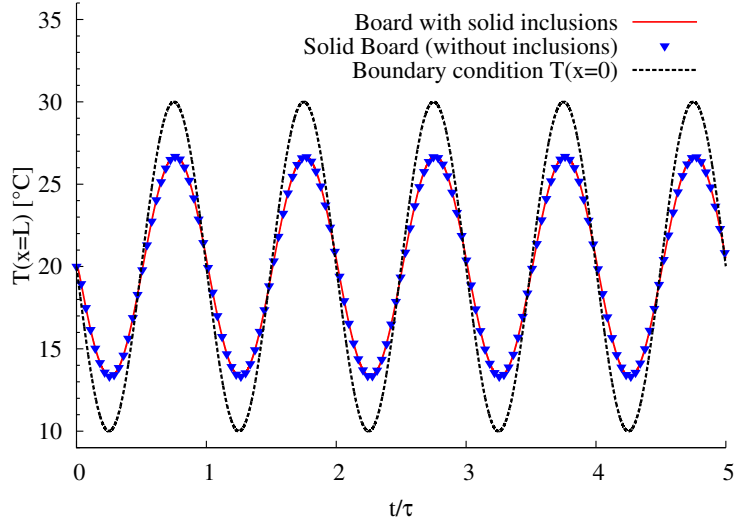


Figure 2: *Test of the model implementation: temperature evolutions at the inner boundary ($x = L$) of a solid wall with and without inclusions. The inclusions have the same properties as the matrix and do not undergo change phase. The temperature of the outer surface ($x = 0$) is also shown (Eq. 6). τ corresponds to one day.*

184 perfect match between the results from the two configurations is observed (see Fig. 2).
 185 As expected, the spheres behave as parts of a homogeneous material.

186 The choice of the adequate mesh size for the two models (board and sphere), repre-
 187 senting the best compromise between accuracy and computation cost, has been done after
 188 three series of computations, where the N , M and dt parameters have been progressively
 189 varied. An example of results provided by such a procedure is given in Fig. 3, for the case
 190 of the parameter N (the number of computational cells within the board thickness) and
 191 for a board thickness of $L = 2.5$ cm. N was varied from 20 to 60. Qualitatively speaking,
 192 the global behavior proves to be the same for all the mesh sizes. Quantitatively, the results
 193 on the coarser grids converge rapidly to the values obtained by the finest one ($N = 60$),
 194 while the relative difference between the values obtained for $N = 60$ and $N = 40$ is always
 195 below 5 %. Thus, the value $N = 40$ was selected. Fig. 4 shows the results of a time step
 196 dependency study. A reasonable choice corresponds to $dt = 10^{-3}$ s since for a larger value
 197 of $dt = 10^{-2}$ s parasite oscillations began to appear. A similar analysis (not detailed here)
 198 allowed us to choose $M = 20$.

199 The two parts of the implemented model were validated separately since no reference
 200 solution is available (to the authors knowledge) for a system of mono-dispersed PCM

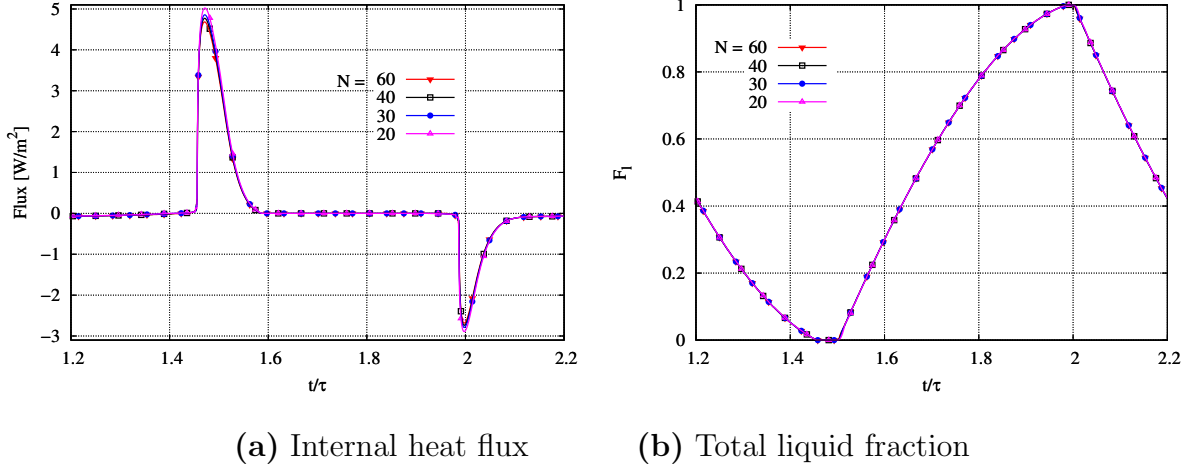


Figure 3: Results obtained for different mesh sizes N of the composite board model with $L = 25$ mm and $\phi = 20$ % ($M = 20$).

201 spheres in a matrix. Thus, the unsteady model of heat conduction through a board
 202 was compared successfully to the classical 1D analytical solution, while the sphere phase
 203 change model was validated against reference solutions given in the literature. Yang and
 204 Zhao [27] proposed a solution to the spherical Stefan problem during solidification. A
 205 finite difference approach combined with explicit and implicit Euler time integration was
 206 developed to solve the Stefan problem involving liquid–solid moving interfaces. The non-
 207 linearities introduced by the moving boundary were simplified by the use of a convenient
 208 transformation of dimensionless variables.

209 They compared their results to those obtained using the iterative analytical series so-
 210 lution of Davis and Hill [28], which is an approximate analytical solution. As an example,
 211 it is possible to compare in Tab.1 the present results with those of Refs. [27] and [28].
 212 The selected quantity represents the number of days t/τ necessary to reach a complete
 213 solidification. It has been obtained for a mesh of $M = 20$ and for different values of the
 214 Stefan number (Ste). The agreement is quite good.

215 3. Results

216 3.1. Effect of board thickness and PCM amount

217 The composite considered in this study consists of a solid matrix formed by a thermally
 218 insulating material containing a dispersed paraffin PCM. The properties of the matrix
 219 material and of the PCM are given in Table 2. Monodisperse spherical PCM are considered

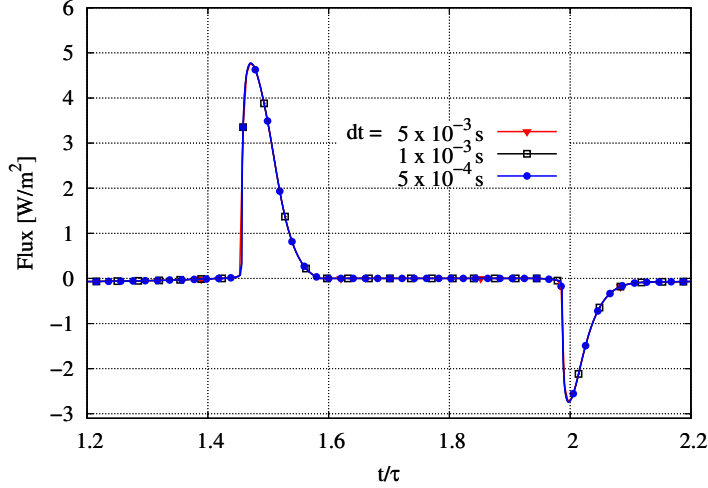


Figure 4: Internal heat flux obtained with different time step values dt for a board of $L = 25$ mm and $\phi = 20$ % ($N = 40$; $M = 20$).

220 with a diameter $d = 100$ μm . The selected values of L are 10, 15, 20, 25, 30 and 50 mm
 221 and the considered values of the fraction of PCM ϕ range from 0 to 50 %. Simulations
 222 represent a total observation time of five days (5τ).

223 In this section, the mean external temperature \bar{T} of Eq. (6) is taken equal to the
 224 melting temperature $\bar{T} = T_m = 20$ °C and the amplitude fixed to $A = 10$ °C (i.e. $T(0, t)$
 225 oscillating between 10 and 30 °C). This simplified signal is chosen so as to limit the
 226 number of parameters of the study (no difference between the mean temperature and the
 227 melting temperature. Usually, the melting point of the phase change material is chosen
 228 in order to match with the average temperature of the climate zone considered). In this
 229 section also, the indoor temperature T_∞ (Eq. 7) was taken equal to T_m as well, for the
 230 sake of simplicity i.e. to avoid the introduction of an additional parameter ($T_m - T_\infty$) in
 231 the analysis. These simplifications help to focus on the role of ϕ and L . The importance
 232 of the gap between the different temperatures is addressed in section 3.4.

233 The propagation of the heat flux within the wall is hampered by both the thermal
 234 resistance of the matrix and by the solid-liquid phase change of the PCM. The temperature
 235 of the inner face of the wall $T(x = L)$ is obtained by the computation and is used to deduce
 236 the heat flux crossing this surface as:

$$\varphi(x = L) = h(T_\infty - T(x = L)) \quad (12)$$

237 In Fig. 5, the evolution of this quantity for four different board thicknesses L and five

Table 1: *Dimensionless time to complete solidification: our results compared to those of Refs. [27] and [28].*

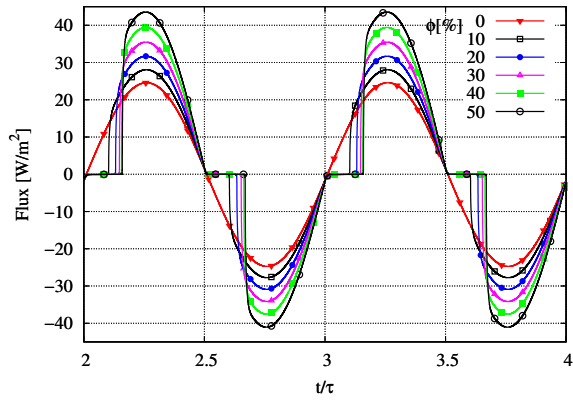
<i>Ste</i> Number	Our Results ($M = 20$)	Yang and Zhao [27]	Davis and Hill [28]
0.01	16.8356	16.8231	16.8327
0.02	8.4932	8.4863	8.4987
0.1	1.809	1.8068	1.8272
0.2	0.9669	0.9654	0.9887
1	0.2750	0.2747	0.2970
2	0.1797	0.1797	0.1988
10	0.0871	0.0881	0.0997

Table 2: *Properties of the studied materials*

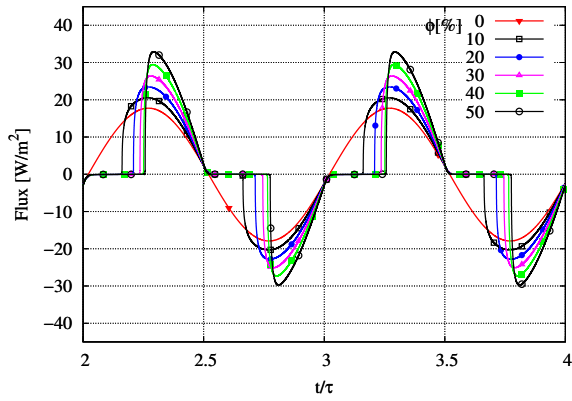
Property	$k [Wm^{-1}K^{-1}]$	$\rho [kg m^{-3}]$	$c_p [J kg^{-1}K^{-1}]$	$L_m [J kg^{-1}]$
Insulating matrix	0.03	900	1200	–
Liquid PCM	0.15	780	2200	2.3×10^5
Solid PCM	0.20	780	2000	–
Cement	1	2000	900	–

238 PCM percentages ϕ is given and compared with the case without PCM ($\phi = 0$, PCM
239 free material). It is observed that for the thin board case $L = 10$ mm, and even for high
240 values of ϕ , the effect of the phase change, which stops the propagation of heat towards
241 the inside, is effective for only a short period of time, after which the flux increases
242 rapidly and reaches values higher than that of the flux of the PCM free case. In fact,
243 at the end of the phase change, the one-phase PCM (solid or liquid) has a much higher
244 thermal conductivity than that of the matrix (see Tab.2), the effective conductivity of
245 the composite being the more important as ϕ is higher. For thicker walls ($L = 15$ and
246 20 mm), the time interval during which the phase change occurs is longer, delaying the
247 moment at which the wall becomes purely conductive and that occurs after the reversal
248 of the external temperature signal, which limits the negative impact of the higher PCM
249 conductivity.

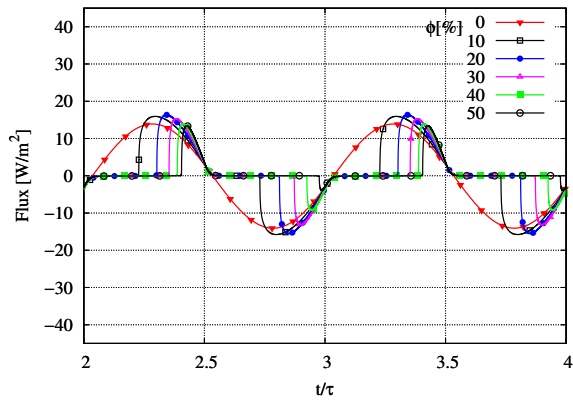
250 Beyond $L \geq 25$ mm and for some values of ϕ ($\geq 20\%$), the phase change process
251 remains incomplete during a whole cycle and along the wall thickness. As a consequence,
252 no heat flux crosses the wall during the whole process. The presence within the wall of a



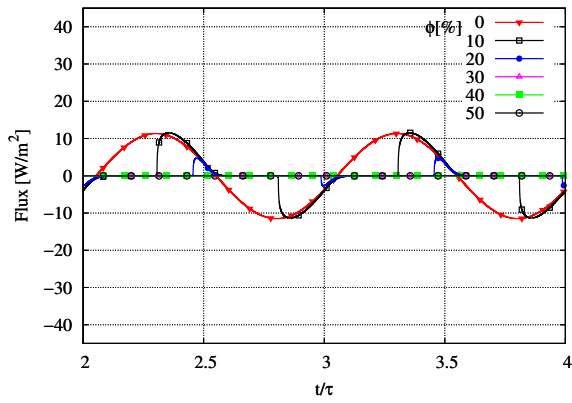
$L = 10 \text{ mm}$



$L = 15 \text{ mm}$



$L = 20 \text{ mm}$



$L = 25 \text{ mm}$

Figure 5: Heat flux crossing walls of thickness equal to 10, 15, 20 and 25 mm and with different PCM percentages ϕ .

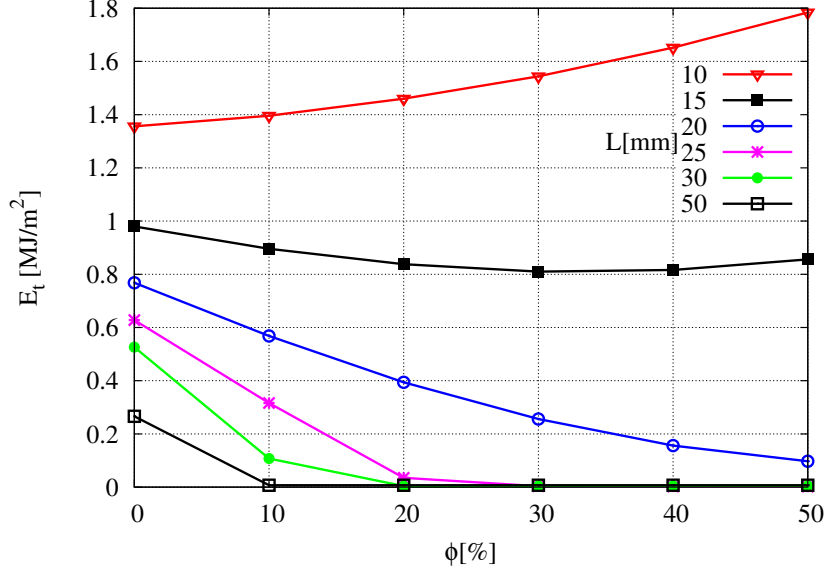


Figure 6: Cumulative total energy (Eq. 13) crossing the indoor surface of the wall in both directions for different thicknesses and different PCM percentages.

253 phase change front (i.e. a zone where the PCM spheres are in a two-phase state) acts as
 254 a thermal barrier.

255 In order to give a comparison of the behavior of a large number of possible (L, ϕ)
 256 combinations, a unique average quantity E_t is defined. It represents the daily total energy
 257 that crosses a unit area of the inner wall surface in both directions (averaged over a 5-day
 258 period):

$$E_t = \frac{1}{5} \int_0^{5\tau} |\varphi(x=L)| dt = \frac{1}{5} \int_0^{5\tau} |h(T_\infty - T(x=L))| dt \quad (13)$$

259 Thus, E_t is the theoretical energy needed to counterbalance (by heating or cooling) the
 260 effect of heat fluxes crossing the wall. This quantity is given in Fig. 6 for a wide range of
 261 L and ϕ values. By analyzing in this figure the behavior of the $L = 10$ mm board, it can
 262 be seen that the addition of PCM to the matrix, even at a low percentage, has a negative
 263 effect on its thermal insulation behavior, since its performances for $\phi > 0$ are lower than
 264 those obtained for the PCM free case ($\phi = 0$).

265 For $L = 15$ mm, the addition of a percentage of PCM such as $\phi \leq 30\%$ has a positive
 266 effect that increases as ϕ is increased, up to a value of $\phi \simeq 30\%$. Beyond this value
 267 the insulation performances of the wall decrease, yet remaining better than those of a
 268 PCM free board. Thus, for this thickness, the addition of such a high percentage of PCM
 269 ($\phi > 30\%$) is not justified, at least for cost reasons, since better performances can be

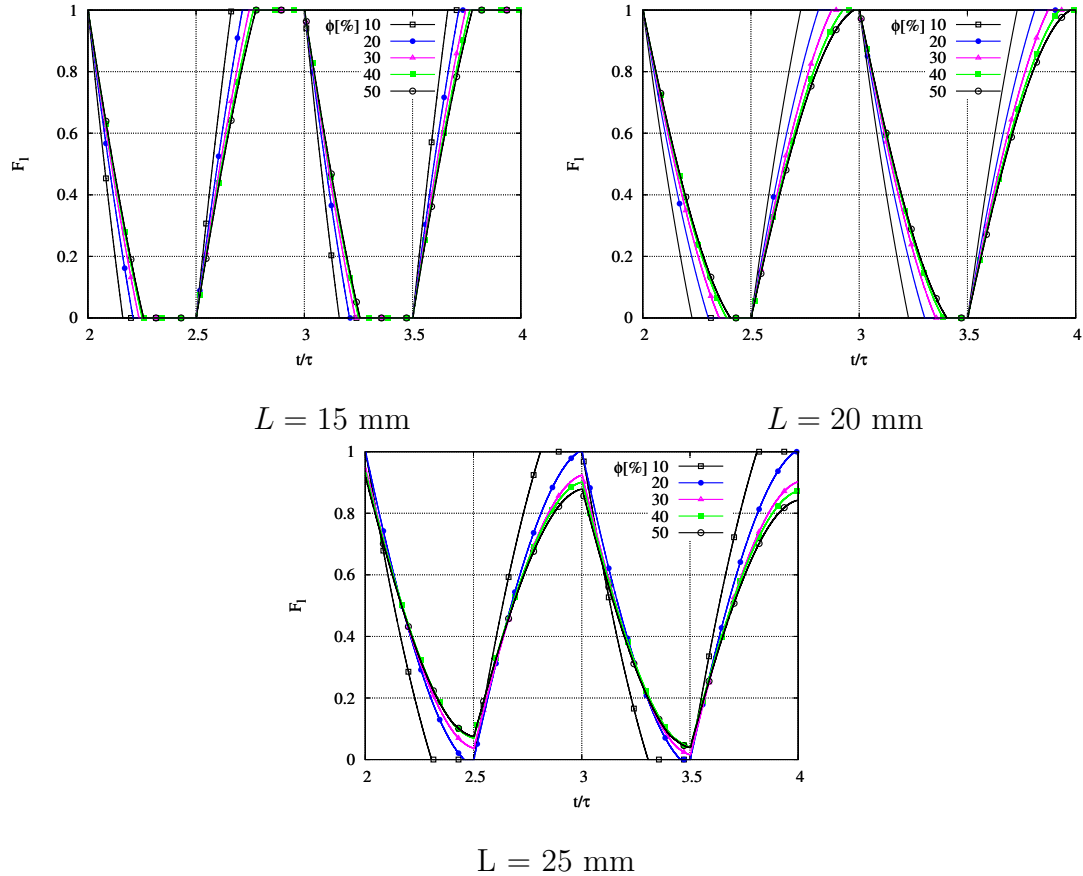


Figure 7: Total liquid fraction of the dispersed PCM for 3 wall thicknesses $L = 15, 20$ and 25 mm.

270 achieved by slightly increasing the thickness (see $L = 20$ mm and $\phi = 0$). The board of
 271 thickness $L = 20$ mm exhibits performances that improve continuously with the increase
 272 of the amount of PCM, but without reaching the limit of $E_t = 0$ (permanent thermal
 273 barrier). This limit is almost reached by the board of $L = 25$ mm from $\phi \geq 20\%$.

274 Actually, as seen from the curves of Fig. 7, which give the total liquid fraction of PCM
 275 of all the inclusions of the composite board, for $L = 20$ mm, complete solidification and
 276 fusion occur for all ϕ values at every cycle. On the other hand, for $L = 25$ mm and from
 277 $\phi > 20\%$, the phase change of the PCM is not complete at every cycle, which indicates
 278 the permanent presence of a two-phase zone at $T = T_m$ that sweeps through the wall
 279 thickness between $x = 0$ and L without disappearing. Therefore, it is very interesting to
 280 choose the conditions that keep as long as possible the PCM in a two-phase state. Of
 281 course, this is only possible for situations with very regular cyclic thermal loads.

282 For values of $L < 20$ mm (see Fig. 6), performance improvement necessarily involves
 283 an increase of the thickness L . In contrast, from $L = 20$ mm, better performances (in

284 comparison to a pure insulation) can be achieved with only 10 % of PCM compared to
285 that obtained when using a 25 mm-thick PCM free board. With a PCM percentage of 40
286 %, the performances of a board of $L = 50$ mm of pure insulating material (i.e. PCM free)
287 are recovered. So, in these conditions, if space-saving constraints arise, a pure insulating
288 material can be advantageously replaced by a thinner insulating material containing a
289 dispersed PCM.

290 *3.2. Dispersion in a cement-based wall*

291 The system studied in the previous section consists of the dispersion of PCM in a less
292 conducting material (insulating material). Thus, the presence of the PCM has a positive
293 effect as long as the phase change is in progress, since at the end of the phase change, the
294 conductivity of the composite material becomes higher than that of the matrix material.
295 Hence, it is interesting to compare this behavior to the one of a more frequently used
296 system that consists of the dispersion of the PCM within a higher thermal conducting
297 building material such as a mortar or a cement wall [29]. For this purpose, numerical
298 experimentations were conducted concerning such a wall by replacing the thermophys-
299 ical properties of the insulating matrix by those of a typical cement material exhibiting
300 higher thermal conductivity (see Tab. 2). Fig. 8 gives the evolution of the heat flux at
301 internal wall surface and of the global liquid fraction for two wall thicknesses and different
302 percentages of PCM.

303 The addition of PCM to this cement wall has a positive effect on the reduction of the
304 heat flux crossing the wall whatever the percentage and the wall thickness. Obviously,
305 the more PCM is added the more pronounced is this effect. Since the PCM conductivity
306 is below that of the cement, there is no inversion of the effect after the end of the phase
307 change process, as it is the case for the insulation matrix (see Fig. 5). However, contrarily
308 to an insulating material, the dispersion of PCM in a cement wall implies that aspects of
309 material strength should be examined, because these types of material are usually used
310 in the structure. The non inversion of the effect of PCM inclusion, can also be obtained
311 for other building materials such as gypsum boards since their thermal conductivity is
312 comparable to that of PCM.

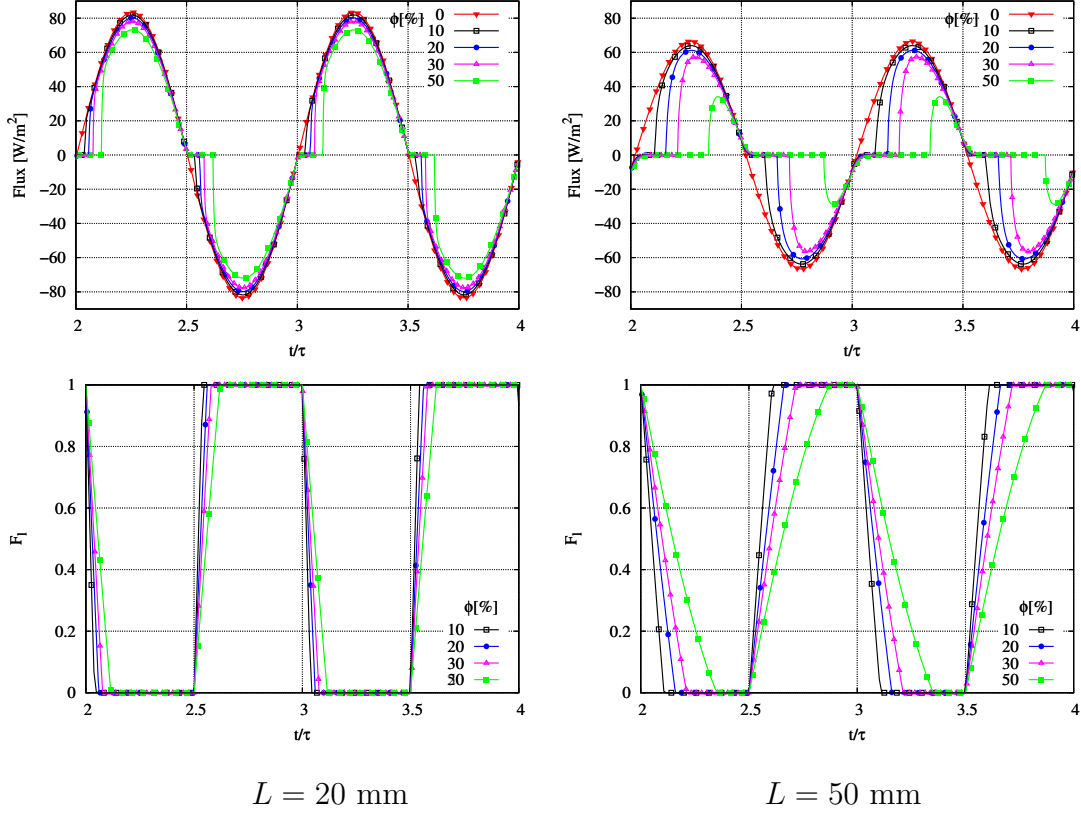


Figure 8: Heat flux (top) crossing a cement wall and total liquid fraction (bottom) of the dispersed PCM for wall thicknesses of 20 and 50 mm with different PCM percentages ϕ .

3.3. Effect of small scale stochastic fluctuations of the external temperature

The results presented above were obtained for a smooth sinusoidal variation of the external temperature boundary condition. In the following, the sensitivity of these results to the presence of small fluctuations of the external temperature signal is examined. These fluctuations are supposed to mimick the indirect effects that external conditions modifications (clouds passage or/and wind speed and direction fluctuations for example) could exert on the external wall temperature. To that end, the temperature signal $T(t)$ is expressed as the sum of three terms $T(t) = \bar{T} + T'_p(t) + T'_s(t)$, with \bar{T} being the temporal mean value, T'_p the periodic (sinusoidal) variation and T'_s a stochastic fluctuation. The last one is obtained by resolving a stochastic differential equation of the Langevin's type [30], that writes as:

$$dT'_s(t) = \frac{-T'_s(t)dt}{\Lambda_T} + \sigma_{T'_s} \sqrt{\frac{2}{\Lambda_T}} dW_t \quad (14)$$

where W_t represents a Wiener's process. The initial condition $T'_s(0)$ is chosen as a Gaussian random variable having a zero mean value and a variance $\sigma_{T'_s}^2$. The numerical solution of

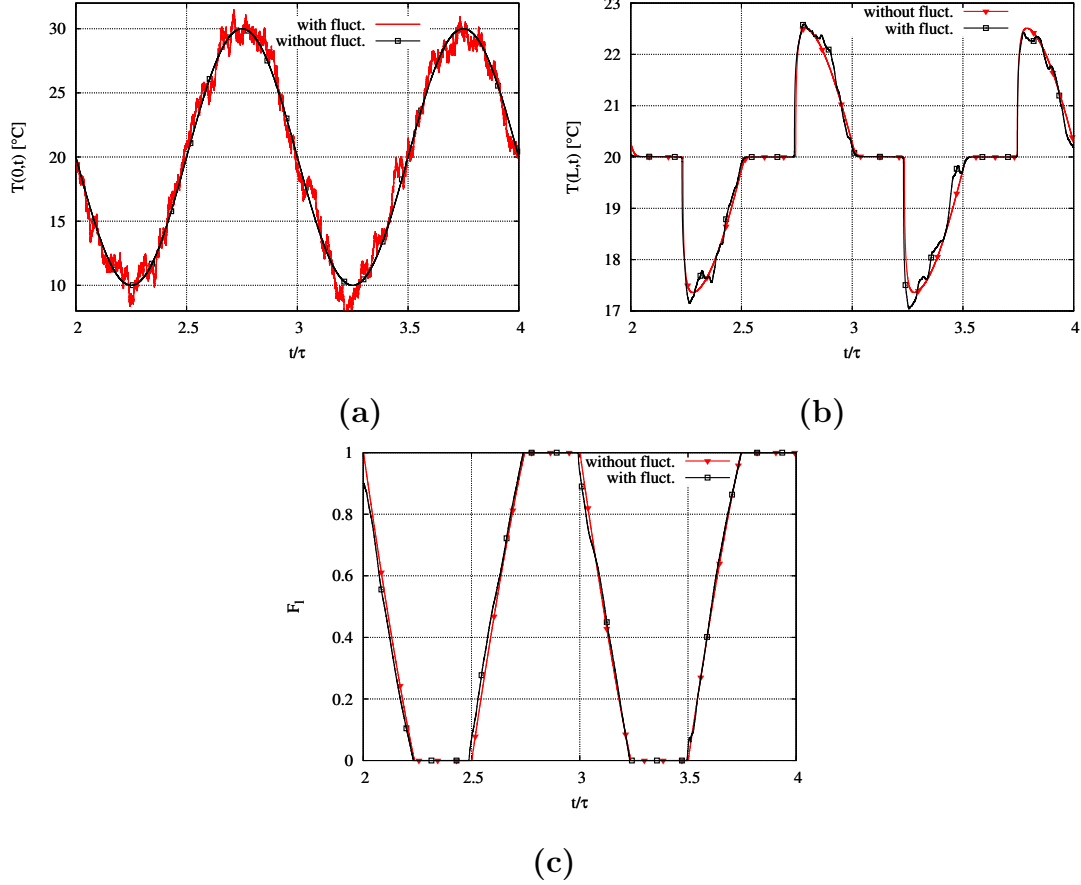


Figure 9: The external temperature signal with superimposed small scale stochastic fluctuations (a), time evolution of the corresponding temperature at the inner surface $x = L$ for a board of thickness $L = 15$ mm and for $\phi = 30\%$ (b) and the evolution of the total liquid fraction (c). The case of an insulating matrix is considered here.

326 these equation is obtained using the “hybrid” method [31] given as:

$$T'_s(t + \Delta t) = \exp\left(-\frac{\Delta t}{\Lambda_T}\right) T'_s(t) + \sigma_{T'_s} \sqrt{1 - \exp\left(-\frac{2\Delta t}{\Lambda_T}\right)} \omega(t) \quad (15)$$

327 where $\omega(t)$ denotes an independent random normal variable of zero mean value and vari-
 328 ance unity i.e. $\omega(t) \in N(0, 1)$. Following Wilson and Zhuang [32], the choice of $\Delta t = \frac{\Lambda_T}{10}$
 329 leads to a discrepancy error less than 2 % when compared to the theoretical Gaussian
 330 probability density function of T'_s .

331 Fig. 9 displays the signal obtained by the above-mentioned method for the parameters
 332 $\Lambda_T = 1800$ s (an integral time scale representative for instance of that of the passage of
 333 clouds) and $\sigma_{T'_s} = 0.9$ (representing the rms amplitude of the fluctuations) and gives the
 334 temperature evolution at the inner surface of the wall obtained when the signal is applied
 335 as an external boundary condition.

336 It is clear that for the conditions considered, the sensitivity of the thermal behavior
 337 of the board to the presence of small-scale fluctuations in the outside temperature is
 338 relatively weak, and its impact on both temporal variation of inner wall temperature
 339 ($x = L$) and total liquid fraction F_l is marginal.

340 Thus, subject to confirmation of the relevance of the generated fluctuations, these
 341 results indicate that using a purely harmonic outside temperature signal is sufficient to
 342 account for the dynamics of the thermal behavior of the wall.

343 3.4. Effect of seasonal weather (winter/summer)

344 Using a composite board as an insulation implies that this material is integrated to
 345 a wall or a building envelope on a yearly basis, and as a consequence, its integration
 346 should lead to an overall positive budget over the passing seasons. Thus, the choice of the
 347 melting temperature of the PCM has a crucial importance. In this study, the question put
 348 forward is the following: “For which conditions is it interesting to replace a pure insulation
 349 board (i.e. PCM free) by a PCM-composite one having the same thickness?”. So, the
 350 question is not about the relevance of superimposing an additional PCM-composite board
 351 to a wall. Furthermore, the question of the cost of materials is not addressed, only the
 352 energetic point of view is dealt with.

353 In the present study, the thermal behavior of a PCM-free material and that of a
 354 composite one are compared during two typical days representing summer and winter
 355 seasons, respectively. The corresponding external temperature variations were taken as:

$$356 \text{ Summer: } T(x = 0, t) = 27 - 7 \sin(2\pi t/\tau) \quad [^\circ\text{C}] \quad (16)$$

$$\text{Winter: } T(x = 0, t) = 5 - 7 \sin(2\pi t/\tau) \quad [^\circ\text{C}] \quad (17)$$

357 Thus, the same amplitude is taken for the two signals (7 °C) while the mean tem-
 358 peratures are 27 °C and 5 °C for summer and winter days, respectively. The indoor
 359 temperatures was chosen to be 26 °C and 20 °C which are close to the standard settings
 360 for HVAC systems for summer and winter seasons. We note that contrarily to the pre-
 361 vious sections, the mean temperatures are here different from the indoor temperatures,
 362 particularly for the winter day. The gap with the melting temperature is analyzed here
 363 by studying the behavior of PCMs having different T_m temperatures. This analysis was
 364 done for a unique board ($L = 25$ mm and $\phi = 20$ %) whose characteristics were chosen

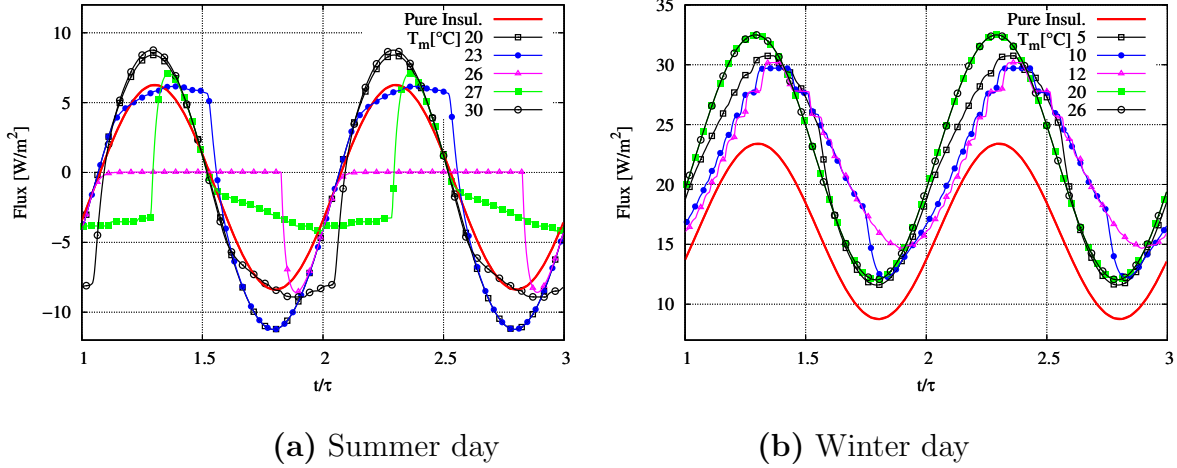


Figure 10: Heat flux crossing the internal surface of a board ($L = 25$ mm, $\phi = 20$ %) with PCMs of different T_m and during typical summer and winter days.

365 using the results of Fig. 6. Thus, the selected board has the minimal L and ϕ values that
 366 yield an almost null crossing energy E_t .

367 The results presented in Fig. 10 give the time evolution of the heat flux crossing the
 368 indoor side of the board for the two typical days considered. For the summer day, the
 369 melting temperatures are ranging from 20 to 30 °C and the results are compared to the
 370 case of a PCM free material ($\phi = 0$ %). The whole crossing energies per day E_t (Eq. 13)
 371 are summarised in Fig. 11(a). In these figures, it can be noticed that the case of $T_m = 26$
 372 °C (equal to the indoor target temperature) gives the best results, while the case $T_m = 27$
 373 °C (equal to the mean external temperature) behaves worse but remains better than all
 374 other T_m values, whose results are even worse than those obtained with the PCM free
 375 board ($\phi = 0$ %, Fig. 11(a)). In Fig. 12(a), that gives the total liquid fraction of the
 376 PCM, it is observed that for $T_m = 26$ °C and 27 °C comparable amounts of PCM were
 377 solidified/melted respectively (but larger compared to the other PCMs). It is clear that
 378 the best choice for T_m is to be as close as possible to the indoor temperature to maintain
 379 most of the time in the board a uniform temperature zone ($\simeq T_m$), located between the
 380 melting front and the internal surface, that will be limiting the heat flux.

381 For the winter day, none of the T_m choices ranging from 5 to 26 °C perform better
 382 than the PCM free counterpart. All the global results are comparable (Fig. 11(b)) for all
 383 the PCMs, with a slight advantage though for lower melting temperatures. Thus, even
 384 if the phase change process takes place within the board (Fig. 12(b)), the temperature

385 gradient is sufficiently high to generate a more important heat flux related to the higher
 386 conductivity of the PCM-composite.

387 Even if it is clearly not relevant for a winter weather, the value $T_m = 26\text{ }^\circ\text{C}$ has been
 388 retained to have a global overview of the annual behavior of the insulating wall. It appears
 389 that the addition of PCM to an insulating matrix permits to save $2.9 \times 10^5\text{ J/m}^2$ per
 390 summer day, while it causes a loss of $5.34 \times 10^5\text{ J/m}^2$ per winter day. Thus, in order to
 391 have an annual positive budget, compared to a PCM free insulation, this board should
 392 be used in hot climatic zones featuring more summer-like days than winter ones. Results
 393 with similar trends have been reported by Izquierdo-Barrientos et al. [18] and Ye et al.
 394 [33].

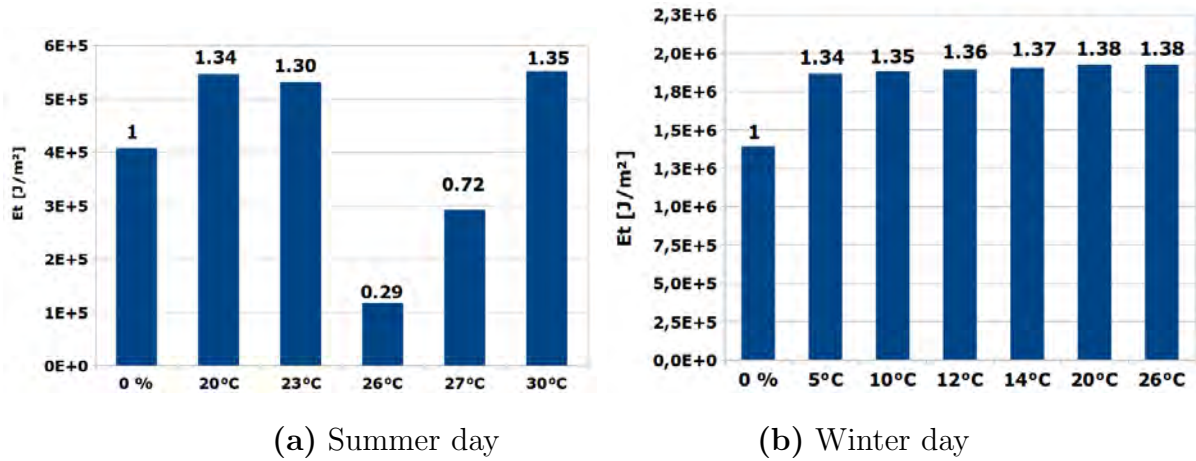


Figure 11: Cumulative total energy E_t (Eq. 13) crossing the indoor surface of the board in both directions for typical summer and winter days and for different T_m ($L = 25\text{ mm}$, $\phi = 20\%$). The values over the bars are the ratios $E_t/E_t(\phi = 0\%)$ that give a comparison to the PCM free case.

395 4. Conclusion

396 In this study, the thermal behavior of a composite material consisting of a micro-
 397 dispersed PCM in an insulating polymer matrix is analyzed. The targeted application
 398 is the thermal insulation and a gain of thermal inertia of a building envelope. By using
 399 two coupled finite volume models, the behavior of the composite board was studied when
 400 submitted to a cyclic harmonic thermal excitation. Different board thicknesses (L) were
 401 considered as well as various volume percentages of PCM inclusions (ϕ). It has been
 402 observed that for a thin board, the introduction of PCM has a negative effect on its
 403 behavior, as it increases its overall thermal conductivity. It was also shown that with

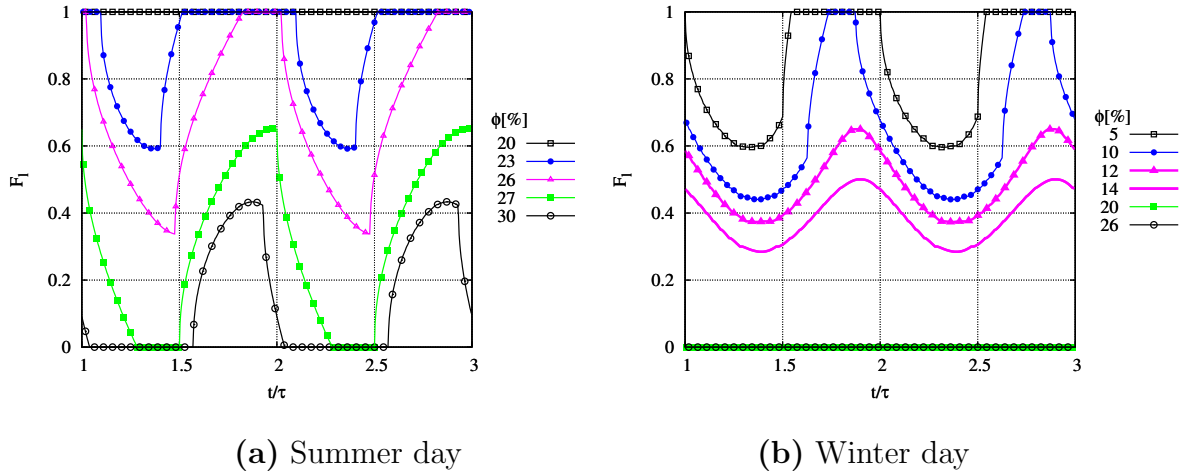


Figure 12: Total liquid fraction of PCM inside a board ($L = 25$ mm, $\phi = 20$ %) with PCMs of different melting temperatures T_m and during typical summer and winter days.

404 some combinations of L and ϕ , it is possible to durably maintain an active phase change
 405 front within the board which then behaves as a genuine thermal barrier. To date, this
 406 feature is not commonly reported. Indeed, it is usually considered that the effectiveness of
 407 the system may be considerably reduced if the PCM is not able to completely solidify or
 408 melt. The results also revealed how pure insulating boards could be favorably replaced by
 409 thinner boards enriched with micro-dispersed PCM allowing the reduction of the overall
 410 thickness of the insulation. It was also shown that the temperature variations within the
 411 material are weakly sensitive to the presence of small scale fluctuations of the external
 412 temperature, representing transient climatic variations. We confirmed also that replacing
 413 a pure insulation (i.e. PCM free) by a PCM-composite insulation should be studied with
 414 care on a yearly basis, since a well behaving material in summer may be a very poor
 415 choice during winter. Thus, the PCM-composite board should be optimized (thickness,
 416 % of PCM, melting temperature, thermal properties of the matrix) taking into account
 417 the climate in which the building is located and the internal and external heat loads.

418 5. References

- 419 [1] S. A. Memon. Phase change materials integrated in building walls: A state of the
 420 art review. *Renewable and Sustainable Energy Reviews*, 31:870–906, 2014.
- 421 [2] J. Kosny, A. Fallahi, N. Shukla, E. Kossecka, and R. Ahbari. Thermal load mitigation

- 422 and passive cooling in residential attics containing PCM-enhanced insulations. *Solar*
423 *Energy*, 108:164–177, 2014.
- 424 [3] S.E. Kalnæs and B.P. Jelle. Phase change materials and products for building ap-
425 plications: A state-of-the-art review and future research opportunities. *Energy and*
426 *Buildings*, 94:150–176, 2015.
- 427 [4] Y. Zhang, G. Zhou, K. Lin, Q. Zhang, and H. Di. Application of latent heat thermal
428 energy storage in buildings: State-of-the-art and outlook. *Building and Environment*,
429 42(6):2197–2209, 2007.
- 430 [5] V.V. Tyagi and D. Buddhi. PCM thermal storage in buildings: a state of art.
431 *Renewable and Sustainable Energy Reviews*, 11(6):1146–1166, 2007.
- 432 [6] N. Soares, J.J. Costa, A.R. Gaspar, and P. Santos. Review of passive PCM latent
433 heat thermal energy storage systems towards buildings’ energy efficiency. *Energy and*
434 *Buildings*, 59:82–103, 2013.
- 435 [7] F. Kuznik, D. David, K. Johannes, and J.-J. Roux. A review on phase change
436 materials integrated in building walls. *Renewable and Sustainable Energy Reviews*,
437 15(1):379–391, 2011.
- 438 [8] M.A. Medina, J.B. King, and Zhang M. On the heat transfer rate reduction of
439 structural insulated panels (SIPs) outfitted with phase change materials (PCMs).
440 *Energy*, pages 667–678, 2008.
- 441 [9] F. Ascione, N. Bianco, R.F. De Masi, F. de’Rossi, and G.P. Vanoli. Energy refurbish-
442 ment of existing buildings through the use of phase change materials: energy savings
443 and indoor comfort in the cooling season. *Applied Energy*, 113:990–1007, 2014.
- 444 [10] C. Castellón, M. Medrano, J. Roca, L.F. Cabeza, M.E. Navarro, A. Fernández,
445 A.I. and Lázaro, and B. Zalba. Effect of microencapsulated phase change material in
446 sandwich panels. *Renewable Energy*, 35(10):2370–2374, 2015.
- 447 [11] V.V. Tyagi, S.C. Kaushik, S.K. Tyagi, and T. Akiyama. Development of phase change
448 materials based microencapsulated technology for buildings: A review. *Renewable*
449 *and Sustainable Energy Reviews*, 15(2):1373–1391, 2011.

- 450 [12] T. Khadiran, M.Z. Hussein, Z. Zainal, and R. Rusli. Encapsulation techniques for
451 organic phase change materials as thermal energy storage medium: A review. *Solar*
452 *Energy Materials and Solar Cells*, 143(7803):78–98, 2015.
- 453 [13] K.A.R. Ismail and J.N.C. Castro. PCM thermal insulation in buildings. *International*
454 *journal of energy research*, 21(14):1281–1296, 1997.
- 455 [14] M. Ahmad, A. Bontemps, H. Sallée, and D. Quenard. Experimental investigation and
456 computer simulation of thermal behaviour of wallboards containing a phase change
457 material. *Energy and Buildings*, 38(4):357–366, 2006.
- 458 [15] F. Kuznik and J. Virgone. Experimental assessment of a phase change material for
459 wall building use. *Applied Energy*, 86(10):2038–2046, 2009.
- 460 [16] A. Castell, I. Martorell, M. Medrano, G. Perez, and L.F. Cabeza. Experimental
461 study of using PCM in brick constructive solutions for passive cooling. *Energy and*
462 *Buildings*, 42(4):534–540, 2010.
- 463 [17] J. Kosny, E. Kossecka, A. Brzezinski, A. Tleoubaev, and D. Yarbrough. Dynamic
464 thermal performance analysis of fiber insulations containing bio-based phase change
465 materials (PCMs). *Energy and Buildings*, 52:122–131, 2012.
- 466 [18] M.A. Izquierdo-Barrientos, J.F. Belmonte, D. Rodríguez-Sánchez, A.E. Molina, and
467 J.A. Almendros-Ibáñez. A numerical study of external building walls containing
468 phase change materials (PCM). *Applied Thermal Engineering*, 47:73–85, 2012.
- 469 [19] L. Cao, D. Su, Y. Tang, G. Fang, and F. Tang. Properties evaluation and applications
470 of thermal energy storage materials in buildings. *Renewable and Sustainable Energy*
471 *Reviews*, 48:500–522, 2015.
- 472 [20] S. Caubet, Y. Le Guer, B. Grassl, K. El Omari, and E. Normandin. A low-energy
473 emulsification batch mixer for concentrated oil-in-water emulsions. *AIChE Journal*,
474 57(1):27–39, 2011.
- 475 [21] C. Forgacz, S. Caubet, Y. Le Guer, B. Grassl, K. El Omari, M. Birot, and H. Deleuze.
476 Synthesis of porous emulsion-templated monoliths using a low-energy emulsification
477 batch mixer. *Journal of Polymers and the Environment*, 21(3):683–691, 2013.

- 478 [22] D.J. Jeffrey. Conduction through a random suspension of spheres. *Proc. R. Soc.*
479 *Lond. A*, 335:355–367, 1973.
- 480 [23] A. M. Thiele, A. Kumar, G. Sant, and L. Pilon. Effective thermal conductivity of
481 three-component composites containing spherical capsules. *International Journal of*
482 *Heat and Mass Transfer*, 73:177–185, 2014.
- 483 [24] X. Zhang, Y. Fan, X. Tao, and K. Yick. Crystallization and prevention of supercooling
484 of microencapsulated n-alkanes. *Journal of Colloid and Interface Science*, 281(2):299–
485 306, 2005.
- 486 [25] V.R. Voller. Fast implicit finite-difference method for the analysis of phase change
487 problems. *Numerical Heat Transfer Part B-Fundamentals*, 17:155–169, 1990.
- 488 [26] K. El Omari, T. Kousksou, and Y. Le Guer. Impact of shape of container on natural
489 convection and melting inside enclosures used for passive cooling of electronic devices.
490 *Applied Thermal Engineering*, 31:3022–3035, 2011.
- 491 [27] J. Yang and C.Y. Zhao. Solidification analysis of a single particle with encapsulated
492 phase change materials. *Applied Thermal Engineering*, 51(1):338–346, 2013.
- 493 [28] G.B. Davis and J.M. Hill. A moving boundary problem for the sphere. *IMA Journal*
494 *of Applied Mathematics*, 29(1):99–111, 1982.
- 495 [29] L.F. Cabeza, C. Castellón, M. Nogués, M. Medrano, Leppers R., and O. Zubillaga.
496 Use of microencapsulated PCM in concrete walls for energy savings. *Energy and*
497 *Buildings*, 39(39):113–119, 2007.
- 498 [30] T. Kousksou and P. Bruel. Encapsulated phase change material under cyclic pulsed
499 heat load. *International Journal of Refrigeration*, 33(8):1648–1656, 2010.
- 500 [31] G.C. Crone. *Parallel Lagrangian models for turbulent transport and chemistry*. PhD
501 thesis, University of Utrecht, 1997.
- 502 [32] J.D. Wilson and Y. Zhuang. Restriction on the timestep to be used in stochastic
503 lagrangian models of turbulent dispersion. *Boundary-Layer Meteorology*, 49(3):309–
504 316, 1989.

505 [33] H. Ye, L. Long, H. Zhang, and R. Zou. The performance evaluation of shape-stabilized
506 phase change materials in building applications using energy saving index. *Applied*
507 *Energy*, 113:1118–1126, 2014.

508 Nomenclature

A	Temperature amplitude (K)
c_p	Specific heat ($J\ kg^{-1}K^{-1}$)
d	PCM inclusions diameter (m)
dt	Integration time step (s)
f	Local liquid fraction of PCM
h	Heat transfer coefficient ($W.m^{-2}.K^{-1}$)
k	Thermal conductivity ($W.m^{-1}.K^{-1}$)
L	Board thickness (m)
L_m	PCM latent heat of melting ($J.kg^{-1}$)
N	Number of control volumes (Matrix discretization)
M	Number of control volumes (PCM inclusion discretization)
r	Radial coordinate in a PCM inclusion (m)
S	V control volume boundary
Ste	Stefan number = $c_p\Delta T/L_m$
s	v control volume boundary
t	Time (s)
T	Temperature (K)
\bar{T}	Time averaged temperature (K)
T'	Temperature fluctuation (K)
v	Control volume (PCM inclusion discretization)
V	Control volume (Matrix discretization)
W_t	Wiener process
x	Spatial coordinate normal to the board (m)
Greek symbols	
ϵ_f	Convergence parameter
Λ_i	Number of PCM inclusions in V_i
Λ_T	Integral time scale (s)

φ	Heat flux ($W.m^{-2}$)
ϕ	PCM volumic fraction
Φ	Source term
ρ	Density ($kg.m^{-3}$)
σ	Standard deviation of the stochastic signal
τ	One-day period
Subscripts	
d	Relative to the dispersed PCM
eff	Effective
<i>i</i>	Control volume index
<i>m</i>	Melting
<i>p</i>	Periodic
<i>s</i>	Stochastic
∞	Relative to indoor conditions
Superscripts	
<i>k</i>	Iteration index
Acronym	
PCM	Phase change material